Modification of condensation nuclei under energy impacts. 1. Ion-stimulated nucleation

V.V. Smirnov, A.V. Savchenko, and V.N. Ivanov

Institute of Experimental Meteorology, Obninsk

Received November 18, 2005

Experiments in different climatic regions of Russia have shown that bipolarly ionizing radiation with intensity from 5 to 10^{12} ion pairs/($cm^3 \cdot s$) independently of its type can stimulate formation of new aerosol particles of 5–100 nm in diameter at energy consumption about 100 eV per 10 molecules of the condensate. These particles have basic properties of cloud condensation nuclei and can participate in modification of cloud processes. Main factors reducing the efficiency of the gas–particle conversion are the relative humidity and air temperature, as well as the content of some gases. The intense and long-term ionization minimizes the effect of these factors. The main factor controlling the new aerosol generation, all other factors the same, is the absorbed energy of ionizing radiation *R*, which threshold value sufficient for generating new particles under natural ionization in the near-surface atmosphere is 10^3 eV/cm^3.

Introduction

The character and intensity of cloud formation processes is strongly determined by the nature and content of cloud condensation and crystallization nuclei (CCN).[1,4,6] The cloud-formation activity of the CCN to a large degree depends on both external conditions and internal factors of the atmospheric aerosol state. Presently, there are no exhaustive and non-contradictory concepts of natural and anthropogenic channels of atmospheric aerosol variability as a whole and CCN in particular. For a long time, the role of reactions of photochemical and radiochemical air–CCN conversion is under uninterrupted discussions.[2,5,6] The prevailing present-day conception is that the contribution of photochemical processes is significant in stratosphere; while for the lower and middle troposphere, any significant reactions of UV-stimulated ionization remain to be unknow.[20,35] In this case, the contribution of background radioactive radiation and cosmic ray emissions can be more significant.[9,10,33,34]

Numerous publications (see reviews in Refs. 23, 28, and 32) present descriptions of intensive emission of aerosol of nanometer size in the near-surface layer. The worldwide accepted name of this interesting natural phenomenon, including some domestic publications,[3,23] the nucleation burst, must not delude one about its close connection with cloud processes. Pathways of physical conversion of emitted nanometer nuclei (D = 3–10 nm) into cloud condensation nuclei larger than 100 nm in size are still poorly understood. For instance, the emission of atmospheric nanonuclei is failed to be attributed neither to diurnal behavior of meteorological parameters, nor to solar radiative intensity or concentration of precursor gases SO_x, NO_x, NH_3, etc.[17,18]

It is accepted (see, for example, Ref. 4) that water droplet clouds and fogs have a typical water vapor supersaturation S = 0.01–0.1%. In this interval, background aerosol particles larger than 0.1 μm in diameter are activated. In free troposphere, the concentration of condensation nuclei with initial diameters more than 0.1 μm falls in the range 200–1000 cm^{-3}, which is comparable with droplet concentration in developing warm clouds.[26]

This explains the well-known "vulnerability" and dependence of cloud formation processes on the state of aerosol component. For instance, marked reduction of CCN concentration leads to decrease of the initial droplet concentration in the cloud. This results in decrease in rates of coagulation growth and precipitation formation. The same effect takes place at too high CCN concentration. When the cloud medium is enriched with active nuclei, current supersaturation is reduced and many small droplets are formed.

Also, the situation with crystallization nuclei is unstable, because their concentration is usually 10^2–10^4 times lower than CCN concentration, therefore the natural clouds predominately exist in the supercooled droplet state. At the same time, there appears a principle possibility to activate or suppress artificially the precipitation formation processes.

These facts stimulated the authors to deeper research into the role of energy factor in the observed variability of cloud condensation and crystallization nuclei. In this first publication we confine ourselves to the following key questions:

1. Is there any influence of the type of ionizing radiation on the degree of the gas–aerosol conversion?

2. What, if any, are the lower and upper energy limits of the conversion?

0235-6880/06/05 359-08 $02.00 © 2006 Institute of Atmospheric Optics

3. How do main meteorological factors, namely, relative humidity, temperature, pressure, etc., influence the conversion processes?

4. How strong, if at all possible, is the influence of atmospheric electricity elements, in particular, the ion-formation intensity, atmospheric ion concentration, and electric field intensity on the conversion processes?

1. On energy perturbation levels of troposphere characteristics

We begin with clarifying what is meant by troposphere perturbation, as well as what perturbation levels or amplitudes are of concern. It is also useful to define which tropospheric constituents may undergo perturbations of natural and anthropogenic origin and compare the expected perturbation levels with environmental standards. The available information[1,9,10,16] is summarized in Table 1.

Based on analysis of these data it is possible, even without discussion of physical and technical principles of perturbations, to draw two preliminary conclusions. First, electrical air constituents are more sensitive to anthropogenic impacts on local scales (first five rows of Table 1). The results of monitoring in 30-km zone of the Chernobyl disaster experimentally confirm this conclusion.[9,11] Second, the potentialities of human intervention into individual cloud-formation processes through changing the concentration and activity of condensation and crystallization nuclei are quite large. This explains the interest to symbiosis of perturbations in electrical and aerosol air states.

2. Ion-stimulated gas–aerosol conversion

Principal conditions of conversion

The available experimental data on ion-stimulated gas–aerosol conversion are presented in Refs. 11, 14, 16, 31, and 33. Summarizing them, we can formulate the following requirements to radiation characteristics stimulating the gas–aerosol conversion in the near-surface atmosphere.

1. Atmospheric lightweight ions appearing during air ionization are the initial material for construction of aerosol particles. Hence, the first requirement to the working radiation is that the energy of quanta (particles) must exceed the energy of ionization of main air components ($\approx$15 eV) independently of the radiation type (UV, alpha-, beta-, gamma-, neutron, etc.). This condition is necessary but not sufficient.

2. A critical condition for aerosol formation in the ionized gas is the presence of lightweight ions of both polarities, negative and positive. Therefore, the working radiation and gas composition must stimulate the bipolar air ionization. In unipolar ionized air media, stable associates fail to be formed because of action of repelling Coulomb forces.[11]

3. Following the argument from Refs. 7 and 11, the age of lightweight ions is of importance. First, the initial ions with lifetimes of 1–10 ms or less have insufficient time to form the hydrate coating around the molecular ion, and second, fresh molecular ions have the structure of O_2^-, N_2^+, etc., "unsuitable" for formation of a stable cluster.

Coulombian association of young ions of different polarities terminates in charge recombination and neutralization of molecules O_2, N_2, etc. However, at lifetimes of the order of 0.1–1 s and longer, the central ions of O_2, N_2 are replaced in the real atmosphere by molecules of gases SO_x^-, NO_x^-, H_2O^+, etc., having more affinity to electron and proton than molecules O_2 and N_2. Model estimates and mass spectrometry measurements[7,11] suggest that when concentrations of sulfur and nitrogen oxides are not very high, the secondary lightweight ions $SO_x^-(H_2O)_n$, $(H_2O)_n$, $NO_x^-(H_2O)_n$, $NO_x^-HNO_3(H_2O)_n$, $H_2O^+(H_2O)_n$, $NH_3^+(H_2O)_n$, etc. are produced in amounts depending on the content of some minor gases.

The Coulombian association of aged ions of different polarities terminates in formation of stable neutral clusters $H_2SO_x^-(H_2O)_n$, $HNO_3(H_2O)_n$, etc.,[14,31] representing hydrated molecules of a number of basic acids.

Table 1. Characteristic levels of natural and anthropogenic perturbations of air media

Element of air medium	Perturbation levels		
	Natural	Anthropogenic	Standard
Ion formation rate, q, $cm^{-3} \cdot s^{-1}$	3–10	$<10^{12}$	<500
Concentration of lightweight ions $n_{\pm}$, cm^{-3}	100–1000	$< 10^9$	$<10^4$
Coefficient of unipolarity n_-/n_+	1 ± 0.2	$< 10^9$	–
Intensity of electric field E, V/m	100 ± 80	0 ± 10^4	$<10^3$
Electric conductivity of air $C_{\pm}$, fS/m	1–10	$<10^7$	–
Aerosol concentration N, cm^{-3}	10^2–10^5	$<10^8$	10^6
Concentration of cloud condensation nuclei Z, cm^{-3}	10–10^3	$<10^8$	–
Concentration of crystallization nuclei Z_{cr}, cm^{-3}	10^{-3}–1	$<10^6$	–
Concentration of gases O_3 / NO_x, ppbv	< 50/ 5	>100/10	15/70

Environmental effect

Gas admixtures. Based on the above data, we can anticipate a significant role of gas admixtures affecting the structure and chemical composition of lightweight ions. The data of quantitative analysis of ion-stimulated nucleation products are still fragmentary. However, it has been found that there is a considerable set of chemical species which either sharply enhance the rates of gas-aerosol conversion (sulfur and nitrogen oxides, vapor of sulfur, nitrogen, hydrochloric, and other acids, ammonium, etc.) or reduce them to zero (halogens, vapor of most oil products, etc.).[16] Below we will estimate the mass concentration variability of the radiolytic aerosol (RA) during variations of the air gas composition in remote regions.

Electric field. Earlier, it was shown[11] that under laboratory conditions the aerosol generation rate in the bipolarly ionized air can be controlled by fitting the unipolarity coefficient for lightweight air ions, e.g. by imposing the static electric field. In the framework of bipolarity conversion condition this can be explained by the fact that the removal of ion of any polarity is equivalent to removal of ions of both signs. In the real troposphere, mean mobility of lightweight ions of different signs differs by 10–20%, while the natural electric fields in troposphere are weak (about 100 V/m). Therefore, it is considered that they cannot have a marked influence on composition of atmospheric ions and conversion processes. However, the experimental confirmation is still absent.

Air pressure. Laboratory experiments have shown[11] that, as pressure decreases from its standard value to 100 hPa, the rate of new particle growth decreases but nonlinearly (a little slower) under air irradiation by the isotope Pu-239. The shape of particle size distribution function is practically unchanged.

Theoretically, the pressure dependence of conversion parameters is ambiguous. For instance, the mobility of air ions is inversely proportional to the ambient pressure. The mobility of ions determines the characteristic time and rate of recombination, i.e., the increase of generation rate of clusters and nanoparticles in a rarefied air. At the same time, the hydration number, the lightweight ion mass, and the hydration time are proportional to the atmospheric pressure.

Relative air humidity. Figure 1, based on data from Ref. 11, presents dependences of mass concentration M of photo- and radiolytic aerosol particles with diameters from 5 nm to 1 μm on 20–95% variations of the relative humidity of air, entering the ionizer, at $T = 25$°C. A flow heater of air is set at the exit of ionizers, which increases the temperature of air containing new aerosol particles up to 105°C.

From analysis of Fig. 1 we conclude that:

– the function $M = f(H)$ has the maximum in the interval $H = (60 \pm 5)\%$ for Pu-239 source and $H = (45 \pm 5)\%$ for UV one. The minimum was always at $H = (80 \pm 5)\%$;

– the character of $M = f(H)$ for both sources remained the same even on heating the aerosol at the ionizer exit from 25 to 105°C;

– as the relative air humidity exceeded $(80 \pm 5)\%$, the particle mass concentration grew;

– heating of air to a temperature of (70 ± 10)°C caused a partial evaporation of new aerosol particles.

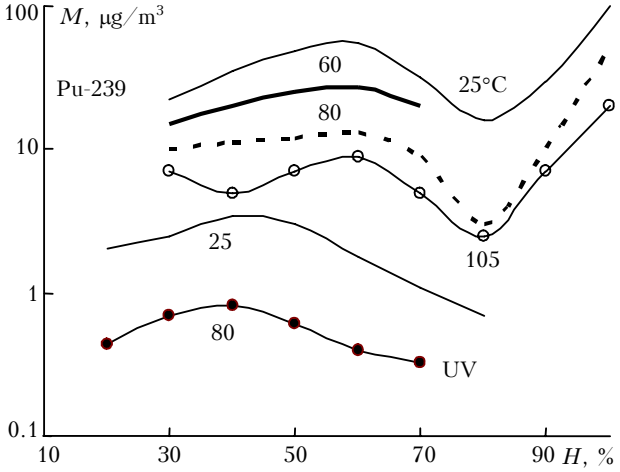

Fig. 1. Influence of the relative humidity H and air temperature T on mass concentration of aerosol particles M, produced during ionization of small volumes of the dust-free air by the isotope Pu-239 ($q = 5 \cdot 10^{10}$ cm$^{-3} \cdot$s^{-1}) and by hard UV ($q = 1.5 \cdot 10^{10}$ cm$^{-3} \cdot$s^{-1}). The exposure time is 100 s.

Of note is the appearance of two maxima in $M(H)$, first observed in Ref. 11. It would be logical to expect a slow growth of new particle mass when H exceeds 60–70%, similar to the character of watering hygroscopic nuclei.[1,4] However, in practice we see a quite sharp (a factor of 2–4) increase of M already at the humidity increase from 30 to 60% and its maximum at $H = (60 \pm 5)\%$ followed by a drop to the initial value and even lower at $H = (80 \pm 5)\%$. It is quite obvious that this effect is not connected with manifestation of the aerosol specific hygroscopicity.

Possibly, the answer is in results of numerical simulation of evolution of negative lightweight air ion.[7] It turns out that as the relative air humidity exceeds 50–60%, the number of water vapor molecules attached to the molecular ion, or the hydration number, may exceed $n = 4 \pm 1$. A coating filled with H_2O molecules is formed around the initial molecular ion O_2^-, which prevents the transition of a free electron to molecules with larger energy of affinity to the electron, in particular, to molecules NO_x, SO_x, etc., so the "aging" of lightweight ions becomes complicated. Formation of neutral clusters and other condensate particles is slowed down, which is just observed in the experiment.

As the relative humidity exceeds 80–85%, the process of watering of new particles becomes prevailing; these particles in the pure air at $H = 50$–60% are droplets of water solution of nitric acid.[31]

In general, in the interval of the exposure time t_0 = 5–7600 s, under standard atmospheric conditions the growth rates of new particle total mass concentration fall in the range dM/dt = = 0.25–2 μg/(m^3·s).

Air temperature. Experiments[11] have shown that a decrease of near-surface air temperature to negative values –(10–20)°C increases the condensate mass by a factor of 2–5. Individual data are presented in Fig. 2. However, in laboratory experiments this tendency was much weaker.

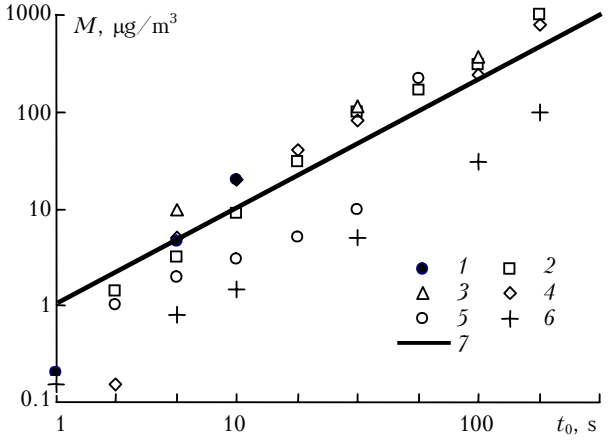

Fig. 2. Influence of the time t_0 of air exposure to isotope Pu-239 ($I \approx 10^{-6}$ A) on the mass concentration M of new aerosols in characteristic climatic-geographic regions: mountains (the Pamirs, 3000 m, September 1989, T = (10 ± 10)°C, H = (50 ± 20)%) (*1*); a sea (Kola Bay, December 1989, T = –(4–10)°C, H = (70 ± 20)%) (*2*); forest-steppe (the Ukraine, region of Chernobyl Power Plant, Junes of 1986 and 1987) (*3*); a desert (Tajikistan, September 1989, T = (25 ± 3)°C, H = (30±10)%) (*4*); a forest (near Moscow, June 1986, T = (20 ± 5)°C, H = (70 ± 20)%) (*5*); a highway (near Obninsk, March of 1986, T = (5 ± 3)°C, H = (80 ± 10)%) (*6*); and calculations by formula (1) (*7*).

Energy factors

From general physical considerations, there must exist an ionizing radiation level, below which the gas–aerosol conversion is not realized. Abundant experimental data (see overviews in Refs. 11 and 16) are obtained through the use of nuclides with the activity many times exceeding the natural level. In recent years, numerous facts of intense emissions of medium-weight ions and aerosol particles of nanometer sizes (D = 3–10 nm) and condensation nuclei were marked in a number of European North regions.[19–21,27,32] Different models of ion-stimulated conversion were used to interpret these results. Data from Refs. 12, 13, 18, 25, and 30 suggest that the above-indicated "recombination" conversion model has made it possible to quantitatively interpret bursts of concentration of medium-weight ions and nanoparticles at a natural ion-formation rate of the order of 5–10 ion pairs in 1 cm^3 per 1 s.

Despite a wide range of ionizers used in the experiments, we failed to clarify the criteria of their efficiency in real near-surface atmospheres. Below we will compare specific expenses of hard UV and alpha-radioactive radiation per unit yield of aerosol matter in characteristic climatic and geographic regions, and compare limiting ionization levels.

Influence of the radiation type

During the field experiment, the disperse composition of background aerosol with particles between 5 and 10 nm in size and the aerosol formed upon irradiating air in flow chambers of 400 and 1000 cm^3 volume have been systematically measured. A substrate of the isotope Pu-239 was located on the side surface of the 400 cm^3 chamber. The base of the second ionizer was a quartz tube of 5 cm in diameter and 22 cm in length. At a 2-cm distance from the tube, a quartz lamp of the PRK type with hard "ionizing" lines in the emission spectrum was mounted. Photoelectric spectrometer of aerosols (PC-218, Royco Inc., USA), and electrical analyzer (3030, Thermo Systems Inc., USA), as well as analyzers of atmospheric ion mobility were used in measurements of characteristics of aerosol sized between 1 and 5 μm.[15,29]

Spectrometer of supersaturation cloud nuclei contained a variable-temperature flow chamber and a photoelectric counter of the AZ type. The instruments were located at a height of 1.5 m above the ground surface. Air entered the measuring instruments either directly or through the ionizers with a FPP-15 cloth filter at the entry.

The measurements of the number concentration N and the mass concentration M of radiolytic and photolytic aerosol at some values of the absorbed radiation dose R, as well as of the background aerosol in Moscow suburbs are presented in Table 2. Their comparison reveals the following main tendencies:

1. The mass concentration of the artificial aerosol is determined by the absorbed specific energy R of radiation rather than by the emission type. Its increase by approximately a factor of 10 is seen to lead to a growth of the mass concentration from 2.7 to 15 μm/m^3. In episodes with emissions of nanoparticles under natural ionization (with R being $5 \cdot 10^3$ times lower than in ionizers), the mass concentration of new particles reached values also approximately by a factor of $5 \cdot 10^3$ lower: $M \approx$ $\approx 6 \cdot 10^{-4}$ μm/m^3.

2. In comparison with the mean value of the background aerosol total mass concentration near Moscow (M = 50–100 μg/m^3),[8] the observed M values at the artificial ionization were much lower. However, it is necessary to keep in mind the 80–90% contribution of the coarse-mode fraction (D > 0.5 μm) into the mass concentration of the near-surface background aerosol. In the case of radiolytic aerosol, 80–90% of its mass make the fine-mode particles with diameters less than 0.1 μm.[10]

Table 2. Characteristic values of the number concentration, its relative variability, and mass concentration of aerosol particles of $D = 5-100$ nm

Type of radiation	α-emission Pu-239		Hard UV	Background radiation
Number concentration N, cm^{-3}	$2 \cdot 10^4$	$4 \cdot 10^4$	$3 \cdot 10^5$	$4 \cdot 10^3$
Variability $\delta N/N$, %	30	15.3	60	16
Mass concentration M, $\mu m/m^3$	2.7	15	8	10^{-4}
Absorbed energy R, eV/cm^3	$3 \cdot 10^{12}$	$5 \cdot 10^{13}$	10^{13}	$3 \cdot 10^6$
Intensity of ion formation, q, $cm^{-3} \cdot s^{-1}$	$1.5 \cdot 10^{10}$	$2.5 \cdot 10^{11}$	$5 \cdot 10^{10}$	5.5 ± 0.5
Exposure time t_0, s	6	6	6	$2 \cdot 10^4$

Note. Particles are formed under impact of individual sources of bipolar ionization. The relative air humidity is (70 ± 20)%, and temperature is (21 ± 10)°C. A forested terrain near Obninsk, Kaluzhskaya Region, summer 1996. Data for conditions of background radiation in the episode with emission of nanoparticles are taken from Ref. 17.

3. The R dependence of N has a maximum at $R \sim 10^{13}$ eV/cm^3. Further R growth leads to decrease of the fraction of small particles because of their faster coagulation sink on the newly formed larger-sized nuclei.

4. Somewhat larger variations of the concentration variability $\delta N/N$ for background aerosol than for the artificial one are due not to the mechanical mixing, but, more likely, to some other factors, such as the concentration variability of precursor gases.[16]

Influence of absorbed radiative energy

To determine the character of R dependence of the radiolytic aerosol total yield M and to estimate the influence on the dependence of geographic and meteorological factors, we measured the disperse composition of new aerosols at the exit of the Pu-239 isotope ionizer in regions with continental, maritime, mountainous, and arid climate.

The measurements are summarized in Fig. 2. To pass from data of the dispersion analysis to the mass concentration M, we used the aerosol matter density $\rho = 1$ g/cm^3. The theoretical dependence of maximum possible mass concentration M ($\mu m/m^3$) of the radiolytic aerosol on the productivity and time of ionizer action is shown as well[11]:

$$M = 3 \cdot 10^5 \, q m_i t_0, \qquad (1)$$

where $q = I/eB \approx 1.5 \cdot 10^{10}$ $cm^{-3} \cdot s^{-1}$ is the intensity of ion formation; I is the isotope ionization current; $e = 1.6 \cdot 10^{-19}$ C is the elementary charge; $m_i = m_+ + m_- \sim 2 \cdot 10^{-22}$ g is the sum of average masses of negative and positive aged lightweight ions; $B = 400$ cm^3 is the ionizer volume; and t_0 is the exposure time. As is seen, at t_0 between 1 and 10^3 s the function $M = At_0$ is linear (A is the proportionality coefficient varying in the near-surface atmosphere of different regions) in a relatively narrow range: $A = (1.1 \pm 0.3)$ $\mu m/(m^3 \cdot s)$.

Considering measurement errors of the ion current (± 25%) and the aerosol dispersivity (± 20%), it can be concluded that dependence (1) quite adequately describes the kinetics of aerosol matter building-up as the contribution of ionizing energy increases within three orders of magnitude. The experimental data in Fig. 2 make it possible to draw some other interesting conclusions:

1) It was assumed in deriving formula (1) that all ionization-created lightweight ions are consumed for aerosol matter formation. Since data for remote regions with mountainous, steeper, and maritime climate are concentrated near the calculated line (1), it is reasonable to hope that for the given ionizer, with exposure times longer than 10 s the influence of local conditions, including meteorological ones, is insignificant.

2) For forests growing near highways, M values are 10 or more times lower than those calculated by Eq. (1). Gas analysis[31] has shown that characteristic hydrocarbon levels in this case were 5–10 times higher than, for example, in mountainous and polar regions. Hydrocarbon admixtures are shown to reduce the content of nitrogen oxides in air.[11] At longer exposure times, when the own radiochemical mechanism of nitrogen oxide production becomes efficient, the build-up of the condensate accelerates and relation (1) begins to fulfill.

3) For small exposure times $t_0 < 10$ s, M values have a large dispersion independently of the observation region and are always below theoretical predictions (1). Based on the above analysis, we can suppose that main causes of the observed fact are variations in concentration of some admixture gases, relative humidity, and air temperature.

To obtain representative measurements at $R < 3 \cdot 10^{12}$ eV/cm^3, the exposure time had to be increased up to 10^4 s and more. However, in this case, because of volume finiteness of ionizers, we faced a phenomenon of diffusiophoresis of formed ions and nanoparticles, which is difficult to be taken into account. To assess the regularities of conversion at low R, consider Fig. 3 showing measurements of concentration kinetics for medium-weight ions and nanoparticles during their intense emission in spring 2000 at Hiitiala, Finland.[18]

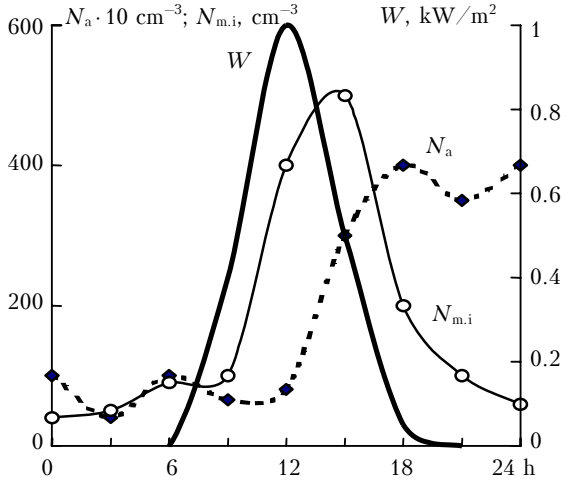

Fig. 3. An example of recorded diurnal variations of concentration of medium-weight ions $N_{m.i}$ and aerosol N_a larger than 3 nm in diameter, as well as total solar radiative flux W in episode with natural emission of new particles at an intensity of their formation of (5.5 ± 0.5) cm$^{-3} \cdot$ s^{-1}. Data are taken from Ref. 17.

As is seen, first (starting from 9 a.m. LT) only emission of medium-weight ions is observed. Around noon, there appear nanoparticles with diameter larger than 3 nm. Increase of their concentration to $N_a = 4000$ cm^{-3} lasts for 5–6 h. By 6 p.m. LT, the mass concentration of nanometer particles M reached 10^{-4} μm/m^3 at a mean cubic diameter of new particles of ~ 4 nm. In approximation of the recombination conversion model, this mass of condensate can be obtained by expending the ionizing energy in a unit volume

$$R = 2q\varepsilon t_0 \approx 3 \cdot 10^6 \text{ eV/cm}^3, \qquad (2)$$

where $q = (5.5 \pm 0.5)$ cm$^{-3} \cdot$ s^{-1} is the natural intensity of ion formation at a given site[22,24]; $\varepsilon \approx 16$ eV is the energy for formation of one lightweight ion; and $t_0 = 2 \cdot 10^4$ s is the exposure time of the studied air mass. The coefficient 2 means formation of two (negative and positive) ions in each ionization event. It follows from formula (2) that under optimal conditions no less than 10 eV of ionizing energy is required for formation of one molecule of the condensate.

Note that the close-to-linear character of the growth of the number concentration N_a for nanoparticles was observed during 6 h, whereas the correlation with solar radiative intensity was absent. After 17–18 LT, the growth of N_a became slower, which is attributed[17] to an intense coagulation growth and enlargement of nanoparticles. At the same time, the volume (mass) concentration was growing monotonically until termination of new aerosol material emission.

In Fig. 4, the measurements for natural and artificial ionization are summarized and compared with calculations by formulas (1) and (2), made in the framework of the recombination conversion model and under assumption that the "ion" resource was totally run out.

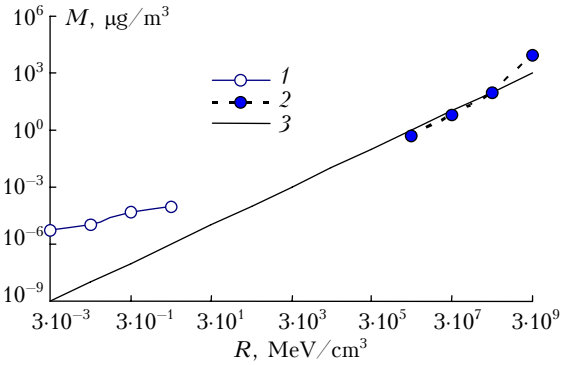

Fig. 4. Mass concentration M of new particles versus specific absorbed energy R of radiation for natural (*1*) and artificial (*2*) air ionization. Calculations (*3*) by formulas (1) and (2).

It is seen that in case of the natural ionization the minimum value of specific absorbed energy $R = 10^3$ eV/cm^3 corresponds to the threshold in new particle formation. This means that all tropospheric depth has quite definite resources for ion-stimulated formation of aerosol particles at characteristic rates of formation of 3–20 ion pairs/(cm$^3 \cdot$ s).

Also of note is a satisfactory correspondence between behaviors of empirical and calculated functions $M(R)$ in a wide energy interval $R = 10^2$–10^9 MeV/cm^3. First, this gives grounds to expect certain generality in the mechanism of gas–aerosol conversion over a wide range of ion formation rates: from natural value, $q = 5$–10 cm$^{-3} \cdot$ s^{-1}, to that obtained at intense ionization, $q = 2.5 \cdot 10^{11}$ cm$^{-3} \cdot$ s^{-1}. Second, there appear physical reasons to think that, other conditions equal, the main factor of the condensate build-up is the absorbed energy of ionizing radiation.

3. Condensation activity of radiolytic nuclei

The above facts on new particle formation under bipolar air ionization in different climatic and geographic zones are necessary but yet insufficient to estimate the influence of these particles on cloud-formation processes. Analysis of experimental data on condensation properties of new particles in the actual atmosphere (not in model one as in Fig. 1) can answer this question.

Field measurements of the relative humidity influence on conditions of new particle formation under ionization by alpha-radioactive and photoionizing radiation are presented in Fig. 5.

It is seen that, as in Fig. 1, the character of aerosol concentration dependence on the relative air humidity H is identical for both types of irradiation: gradual increase of N until the first maximum in the region 50–75%, minimum at $H = (80 \pm 5)$%, and then growth until $H = 95$%. A change of the

absorbed radiative energy by a factor of 15 does not affect these dependences. On the whole, in interval $H = 30–95\%$, variations of radiolytic aerosol concentration reach about (100 ± 50) times, while variations of background aerosol of the same sizes do not exceed a factor of three.

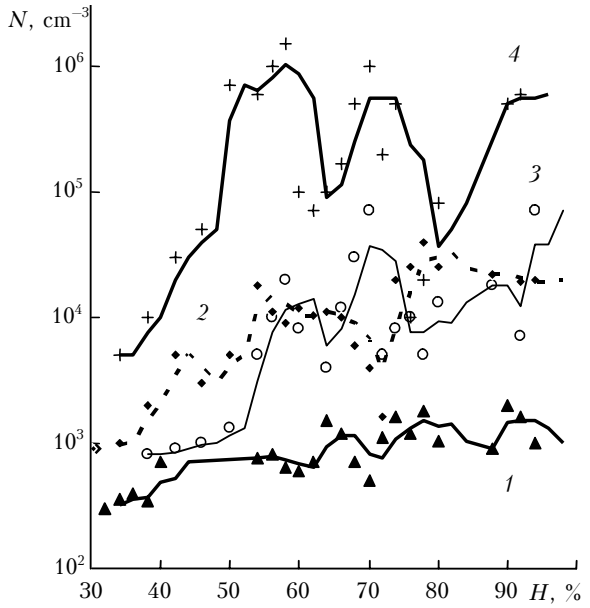

Fig. 5. Number concentrations N of aerosol particles (5–1000 nm) as a function of relative air humidity in the summer period (forested terrain near Moscow): natural aerosol (*1*); after Pu-239 ionization at absorbed energy $R = 7 \cdot 10^{12}$ eV/cm^3 (*2*); the same at $R = 5 \cdot 10^{13}$ eV/cm^3 (*3*); and after hard UV ionization at $R = 10^{12}$ eV/cm^3 (*4*). Lines correspond to the adjacent averaging.

Measurements of radiolytic nuclei spectra at different supersaturations are illustrated in Fig. 6.

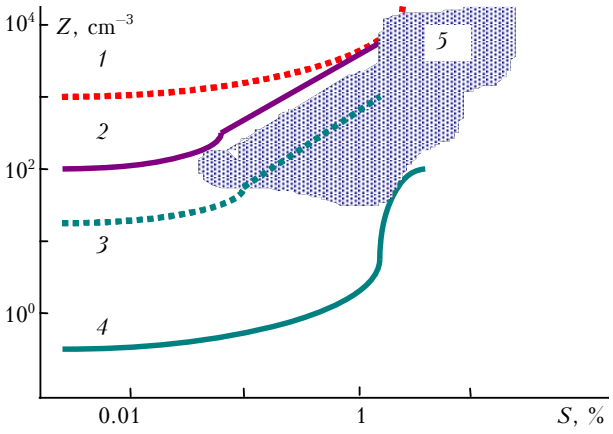

Fig. 6. Integral spectrum of distribution of condensation nuclei concentration Z versus supersaturation S. Episodes with Pu-239 ionization of ambient air (*1–4*) and without ionization (*5*). Measurements of ambient air with background aerosol particles (*1, 3, 5*); air filtered out from background particles (*2, 4*). Curves *1* and *2* correspond to the low limit of drop size measurements ($D = 0.3$ μm), and curves *3* and *4* are for $D > 3$ μm.

We used variable-temperature thermodiffusion chamber with photoelectric counter of droplets. The interval of model supersaturations S for water vapor was 0.01–40%, and interval of measured sizes of grown droplets was 0.3–10 μm. When measuring the activity of background condensation nuclei, the ambient air under normal atmospheric conditions entered the chamber; when measuring the activity of artificial nuclei, either aerosol-free air having passed through the Pu-239 ionizer or the air mixed with background nuclei were used. New particles were generated at $R = 3 \cdot 10^{12}$ eV/cm^3.

For comparison, Figure 6 presents a region of concentration distributions of background nuclei Z, observed in the near-surface atmosphere at $S = 0.1–10\%$. In contrast to the background aerosol, the radiolytic aerosol produced 10 times smaller-sized but quite active nuclei. At a moderate supersaturations ($S = 0.1–10\%$), hazes were formed on these nuclei with droplets of 1000 cm^{-3} concentration and 0.3–3 μm diameters. At low supersaturations ($S < 0.1\%$), the background aerosol had a higher ability to form larger droplets.

Figure 6 also demonstrates that the stay of the background aerosol in ionizer increased its condensation activity as well. Physical aspects of this phenomenon were analyzed in Ref. 9 especially for aerosol processes in 30-km zone of Chernobyl disaster. They suggest a radiolytic nuclei deposition on larger background aerosol particles and increase of their condensation activity.

Thus, aerosol particles formed during ion-stimulated gas–aerosol conversion, have properties of cloud condensation nuclei and can participate in modification of the cloud processes.

Conclusion

1. The bipolar air ionization in the near-surface atmosphere of polar, marine, mountain, forested, and other regions, caused by emissions of isotope Pu-239 and hard ultraviolet radiation with intensity of ion formation between 5 and 10^{12} ion pairs/(cm$^3 \cdot$ s), stimulates the formation of new 5–100 nm aerosol particles. Energy expenses exceed 100 eV per each 10 molecules of the condensate.

2. Specific absorbed energy $R = 10^3$ eV/cm^3 corresponds to experimentally estimated threshold of new particle formation under natural ionization in the near-surface atmosphere. Under other equal conditions, the main factor of new aerosol generation is the absorbed energy of the ionizing radiation. The main factors reducing the gas-particle conversion efficiency are the relative humidity and temperature of air, as well as the content of some admixture gases. Influence of these factors is the least under intense and long-term ionization.

3. In the wide interval of observed energies $R = 10^4–10^{13}$ eV/cm^3, the empirical values of new particle mass concentration are satisfactorily described in framework of the recombination model of ion-stimulated gas–aerosol conversion. This

indicates some generality of the gas–aerosol conversion mechanism at ion formation intensities characteristic both for troposphere ($q = 5–10$ cm$^{-3} \cdot$ s^{-1}) and serious nuclear disasters with emission of nuclides.

4. The aerosol particles formed during bipolar ionization possess main properties of cloud condensation nuclei and can take part in modification of cloud processes.

Acknowledgments

This work is supported by the Russian Foundation for Basic Research (Grants Nos. 04-05-39020 and 04-05-64925).

References

1. L.G. Kachurin, *Physical Fundamentals of Impacts on Atmospheric Processes* (Gidrometeoizdat, Leningrad, 1990), 462 pp.
2. K.Ya. Kondratyev, Atmos. Oceanic Opt. **17**, No. 10, 697–713 (2004).
3. A.A. Lushnikov, in: *Physics of Atmospheric Aerosol* (Dialog-MGU, Moscow, 1999), pp. 207–215.
4. B.J. Mayson, *Physics of Clouds* (Gidrometeoizdat, Leningrad, 1961), 542 pp.
5. D.E. Pozdnyakov, in: *Aerosol and Climate*, ed. by K.Ya. Kondratyev (Gidrometeoizdat, Leningrad, 1991), pp. 141–190.
6. G.B. Rozenberg, Izv. Akad. Nauk SSSR, Ser. Fiz. Atmos. Okeana **18**, No. 11, 1192–1198 (1982).
7. Ya.Yi. Salm, Khimiya Plazmy, Issue 17, 194–217 (1993).
8. V.V. Smirnov, Meteorol. Gidrol., No. 9, 37–49 (2003).
9. V.V. Smirnov, in: *Ecological and Geophysical Aspects of Nuclear Disasters* (Gidrometeoizdat, Moscow, 1992), pp. 117–130.
10. V.V. Smirnov, Izv. Ross. Akad. Nauk, Ser. Fiz, Atmos. Okeana **28**, No. 9, 958–966 (1992).
11. V.V. Smirnov, *Ionization in the Troposphere* (Gidrometeoizdat, St. Petersburg, 1992), 312 pp.
12. V.V. Smirnov, in: *Proceedings of Fifteenth International School of Naval Geology "Geology of Seas and Oceans"* (Moscow, 2003), Vol. 2, pp. 142–143.
13. V.V. Smirnov, Izv. Ros. Akad. Nauk, Ser. Fiz. Atmos. Okeana **41**, No. 6, 1–17 (2005).
14. V.V. Smirnov, Tr. Ins. Eksp. Meteorol., Issue 30(104), 76–106 (1983).
15. V.V. Smirnov and A.V. Savchenko, in: *Proceedings of Fifth Russian Conference on Atmospheric Electricity* (Tranzit IKS, Vladimir, 2003), Vol. 1, pp. 72–75.
16. V.V. Smirnov and A.V. Savchenko, Khimiya v Interesakh Ustoichivogo Razvitiya **13**, No. 5, 649–654 (2005).
17. V.V. Smirnov, J. Salm, J.M. Mäkelä, and J. Paatero, Atmos. Oceanic Opt. **17**, No. 1, 61–69 (2004).
18. V.V. Smirnov, J. Salm, J.M. Mäkelä, and J. Paatero, Meteorol. Gidrol., No. 4, 40–55 (2005).
19. K. Hämeri, M. Väkevä, P. Aalto, M. Kulmala, E. Swietlicki, J. Zhou, W. Seidl, E. Becker, and C.D. O'Dowd, Tellus B **53**, 359–379 (2001).
20. R.G. Harrison and K.L. Aplin, J. Atmos. and Sol.-Terr. Phys. **63**, 1811–1819 (2001).
21. M. Kulmala, J.M. Mäkelä, I.K. Koponen, and L. Pirjola, J. Aerosol Sci. **29**, S567–S568 (1998).
22. L. Laakso, T. Petäjä, K.E.J. Lehtinen, M. Kulmala, J. Paatero, U. Hõrrak, H. Tammet, and J. Joutsensaari, Atmos. Chem. Phys. **4**, 1933–1943 (2004).
23. M. Kulmala, H. Vehkamäki, T. Petäjä, M. Dal Maso, A. Lauri, V.-M. Kerminen, W. Birmili, and P.H. McMurry, J. Aerosol Sci. **35**, No. 2, 143–176 (2004).
24. J.M. Mäkelä, J. Salm, V.V. Smirnov, I. Koponen, J. Paatero, and A.A. Pronin, J. Aerosol Sci. **32**, S149–S150 (2001).
25. J.M. Mäkelä and V.V. Smirnov, in: *Proc. of Intern. Aerosol Conf. to Memory of Prof. A. Sutugin* (Moscow, 2000), pp. 156–157.
26. B.G. Martinsson, G. Frank, and Cederfelt Sven-Inge, Atmos. Res. **50**, Nos. 3–4, 289–315 (1999).
27. C.D. O'Dowd, G. McFiggan, D.J. Creasey, L. Pirjola, C. Hoell, M.H. Smith, B.J. Allan, J.M.C. Plane, D.E. Heard, J.D. Lee, M.J. Pilling, and M. Kulmala, Geophys. Res. Lett. **26**, No. 12, 1707–1710 (1999).
28. V.V. Smirnov, J. Salm, and J.M. Mäkelä, in: *Proc. of Nucleation and Atmospheric Aerosols-2004: 16th Intern. Conf.* (Japan, Kyoto, 2004), pp. 316–319.
29. V.V. Smirnov, in: *Proc. of Intern. Aerosol Conf. to Memory of Prof. A. Sutugin* (Moscow, 2000), pp. 219–220.
30. V.V. Smirnov and J.M. Mäkelä, in: *Proc. 12th Int. Conf. on Atmospheric Electricity* (compiled by S. Chauzy and P. Laroshe) (Versailles, France, 2003), pp. 397–399.
31. V.V. Smirnov, and A.V. Savchenko, in: *Proc of Nucleation and Atmospheric Aerosols-2004: 16th Intern. Conf.* (Japan, Kyoto, 2004), pp. 281–285.
32. V.V. Smirnov and V.V. Shevchenko, in: *Proc. European Aerosol Conf. EAC* (Belgium, Ghent, 2005) (In print).
33. R.P. Turco, F. Yu, and J.-X. Zhao, J. Geophys. Res. **25**, 635–638 (1998).
34. F. Yu and R.P. Turco, J. Geophys Res. **106**, 4797–4814 (2001).
35. F. Yu and R.P. Turco, Geophys. Res. Lett. **27**, No. 6, 883–886 (2000).